Communications on Applied Nonlinear Analysis
ISSN: 1074-133X
Vol 32 No. 6s (2025)

Estimation and Comparison of Seismic Hazard Parameters for National Capital Region of India: using an Updated Earthquake Catalogue

***M. Madhusudhan Reddy[1], Y. Sai Ambika[2], P. Shravya[2], Nageswara Rao Lavuri[3], K. Mahesh Babu[4], Shaik Ummi Salma[5], Chinta Manjusha[6], Salla Arun Tejadhar Reddy[7]**

[1]Assistant Professor, Department of Civil Engineering, Institute of Aeronautical Engineering, Dundigal, Hyderabad, Telangana, India.

[2]UG student, Department of Civil Engineering, Institute of Aeronautical Engineering, Dundigal, Hyderabad, Telangana, India.

[3]Assistant Professor, Department of Electronics and Communication Engineering, CVR College of Engineering, Hyderabad, Telangana, India.

[4]Department of Electronics and Communication Engineering, Sri Venkateswara College of Engineering, Tirupati, Andhra Pradesh, INDIA

[5]Assistant Professor (C), Civil Engineering, UCEN JNTUK Narasaraopet. Andhra Pradesh, India.

[6]Assistant Professor, Electronics and Communication Engineering, Koneru Lakshmaiah Education Foundation, Vaddeswaram, Guntur District, Andhra Pradesh, India.

[7]Assistant Professor, Department of Civil Engineering, Guru Nanak Institute of Technology, Ibrahimpatnam, Hyderabad, Telangana, India.

*Corresponding author: madhu.mrc@gmail.com

Article History:

Received: *23-10-2024*

Revised: *06-12-2024*

Accepted: *13-12-2024*

Abstract:

Delhi, situated in seismic zone class IV with a peak ground acceleration of 0.24 g, is highly prone to seismic activity. This study characterizes the seismicity of the Delhi region (28.70° N and 77.10° E) by considering a radial extent of 350 km around New Delhi. Earthquake data were collected from various sources and literature, resulting in a homogeneous earthquake catalogue with 574 events ranging from 3.0 M_w to 8.6 M_w, spanning the period from 1800 to 2024. Completeness analysis of the catalogue was conducted using the CUVI and Stepp's methods, estimating completeness periods for four magnitude groups: $3.0 \leq M_w \leq 3.99$, $4.0 \leq M_w \leq 4.99$, $5.0 \leq M_w \leq 5.99$, and $M_w \geq 6.0$. Seismic source details, including active faults, faults, and fault tectonics, were digitized using ArcGIS software, resulting in a seismotectonic map featuring four active faults (Pawalgarh Fault, Kotabag Fault, Yamuna Tear, and Kala Amb Tear Fault), 95 fault tectonics, and 3,175 minor and major faults. Seismic hazard parameters such as a-value, b-value, λ_m, M_{max}, and magnitude completeness were computed using standard methods. The a-values ranged from 3.13 to 4.12, and the b-value ranged from 0.65 to 0.83. The M_c value, determined using the Z-map in MATLAB, was found to be 3.5 M_w. This study is significant as it provides a comprehensive and updated catalogue that can be utilized for future hazard analysis of Delhi. The findings of this research will aid in the development of more accurate seismic hazard assessments and preparedness strategies for the National Capital Region, ensuring better mitigation of potential seismic risks.

Keywords: Seismic Hazard, Delhi, Earthquake Catalogue, Seismotectonic Map, Magnitude Completeness, and Hazard Parameters.

1. Introduction

Delhi, the capital city of India, is located in seismic zone IV, indicating a high level of seismic risk. This categorization is part of the seismic zonation map of India, which classifies regions based on their earthquake hazard potential. India's seismic zones are divided into four categories (II to V), with Zone V experiencing the highest seismic activity and Zone II the least [22]. The classification considers factors such as historical earthquake records, tectonic features, and geophysical data. Delhi's placement in Zone IV indicates that the region is prone to severe shaking and potential structural damage during seismic events1. The seismicity of Delhi is closely linked to its geological and tectonic setting. The city lies near the Himalayan seismic belt, one of the most seismically active regions in the world, due to the ongoing convergence between the Indian and Eurasian tectonic plates [25]. This convergence causes significant tectonic stress, leading to frequent seismic activity. The region's complex geological structure includes several major fault lines, such as the Mahendragarh-Dehradun fault, Moradabad fault, and Delhi-Haridwar ridge, which contribute to its high seismic hazard potential [9]. Historically, Delhi has experienced numerous significant earthquakes, which highlight the region's vulnerability to seismic hazards. Notable events include the 1720 Mathura earthquake and the 1960 Delhi earthquake. These historical records, along with modern seismological studies, underscore the importance of continuous monitoring and updating of seismic hazard assessments to effectively mitigate risks [3]. To better understand and mitigate these risks, comprehensive seismic hazard assessments are conducted4. These assessments incorporate geological, seismological, and geotechnical data to estimate the likelihood of various levels of ground shaking and their potential impact on infrastructure [10].

Deterministic seismic hazard assessment (DSHA) and probabilistic seismic hazard assessment (PSHA) are commonly used approaches. DSHA involves analyzing the maximum credible earthquake that could occur in the region, while PSHA considers the probability of different levels of ground shaking over a specified time period. These assessments are crucial for developing earthquake-resistant infrastructure and urban planning. Recent advancements in seismic hazard assessment emphasize the importance of using updated earthquake catalogues [26]. These catalogues, which include recent seismic activity, provide a more accurate representation of the seismic risk. Parameters such as the a-value (seismic activity rate), b-value (slope of the frequency-magnitude distribution), maximum magnitude (M_{max}), and magnitude completeness (M_c) are essential for characterizing the seismicity of a region. The updated catalogues help in refining these parameters, leading to more precise hazard assessments [45,63]. Understanding and accurately mapping the seismic hazards of Delhi is crucial for mitigating risks and enhancing the resilience of infrastructure. The updated earthquake catalogue and the seismotectonic map provide a solid foundation for future seismic hazard assessments and urban planning [29]. These tools enable policymakers, engineers, and planners to design and implement effective earthquake-resistant measures, ensuring the safety and sustainability of the region [64]. The primary objectives of the present study are to develop a seismotectonic map of the Delhi region using an updated earthquake catalogue, to estimate the seismic hazard parameters, and to provide a detailed characterization of the seismicity of Delhi for future hazard analysis. The study area map is shown in Fig. 1.

2. A critical review on the existing literature

A comprehensive understanding of the seismic hazard parameters for Delhi, India, has been developed through numerous studies spanning several decades. A detailed probabilistic seismic hazard analysis for the National Capital Territory (NCT) of Delhi, covering approximately 1,483 km², utilized 515 years of seismic data from 1505 to 2020, encompassing around 4,000 earthquake events with moment magnitudes ranging from 3.5 to 8.0 and focal depths from 5 to 300 km [39]. Their work categorizes Delhi into three seismic zones low, medium, and high hazard based on the likelihood of exceedance at various probabilities over 50 years [41]. This thorough assessment underscores the diverse seismic risks within the region40. An investigation into the seismic hazards in Delhi, focusing on an area of roughly 1,484 km² between latitudes 28.4°N to 28.8°N and longitudes 76.8°E to 77.2°E, employed PSHA methods to develop ground motion prediction equations and assess the likelihood of exceeding specific ground motion levels over different return periods. This study, which analysed earthquake data from 1900 to 2004, concluded that Delhi faces considerable seismic risks due to regional fault systems and the potential for significant ground shaking [5]. Their analysis emphasized the necessity of stringent building regulations and enhanced seismic safety measures to mitigate future risks. Further contributions to understanding Delhi's seismic vulnerability include a microzonation study of the Greater Delhi area, which catalogued 278 seismic events ($M_w \geq 3.0$) from 1720 to 2001 and considered a 300 km radius for a comprehensive assessment24. Their research identified twenty faults responsible for regional seismicity and employed methods such as seismic hazard assessment and site response analysis to produce hazard maps indicating varying degrees of earthquake danger across different zones [28,36]. The study highlighted the influence of local soil characteristics and geological features on the city's susceptibility to earthquake damage, noting that areas with soil amplification and loose sediments are particularly vulnerable.

Using historical earthquake data, another study focused on site-specific ground response analyses to create synthetic accelerograms for various soil conditions. They employed one-dimensional seismic ground response analysis methodologies to predict the impact of seismic waves on different geological formations in Delhi. Their findings revealed that local soil conditions and geological features significantly influence site-specific ground reactions. Regions with more consolidated or rock-like soil exhibited lower levels of ground shaking compared to areas with soft soil and loose sediments. This study highlighted the importance of incorporating site-specific ground response evaluations into seismic hazard assessments and urban development projects to enhance earthquake resilience. A microzonation analysis of Delhi, which encompasses 1,485 km² between latitudes 28.4°N and 28.8°N and longitudes 76.8°E and 77.2°E, considered earthquake records with magnitudes between 6.0 and 7.0, focusing on peak accelerations recommended by the India Meteorological Department. Using one-dimensional site response analysis, they simulated the interaction of seismic waves with various soil types and geological features in Delhi.

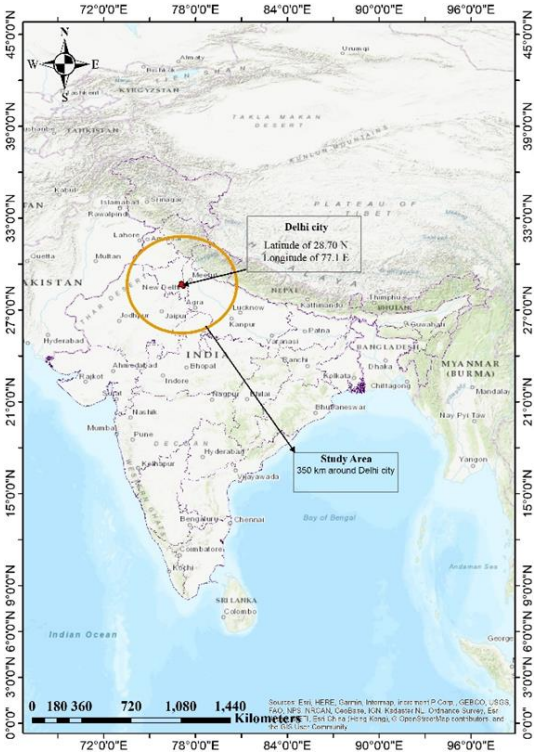

Fig.1: Study area map showing the radial extent of 350 km from Delhi city

The microzonation analysis revealed that several regions of the city are potentially vulnerable to severe ground motion during a magnitude 7.0 earthquake, underscoring the need for appropriate design and construction regulations to ensure structural safety. Another investigation aimed to quantify how seismic wave amplitude diminishes with distance from the source, utilizing regression analysis and empirical attenuation correlations6. Their findings indicated higher attenuation rates in areas with compacted soils and rock formations, which reduce the intensity of ground shaking. This research emphasized that understanding these attenuation features is crucial for accurate seismic hazard estimation and the development of effective mitigation strategies.

A comparative study of the seismic vulnerabilities of Delhi, Dhaka, and Beijing found that Delhi's high population density and numerous older, poorly constructed buildings significantly increase its risk of moderate to severe earthquakes [54]. Rapid urbanization and inadequate infrastructure exacerbate the vulnerability, particularly in densely populated informal settlements. This study underscores the importance of improved infrastructure and strict building codes to mitigate seismic risks in such urban environments. By simulating ground motions from hypothetical moderate-sized earthquakes (M = 5.5 and M = 6.0) likely to occur near the NCR, another study assessed the seismic hazard in Delhi. They analysed various accelerograms with different depths of focus, stress drop values, and geological cross-sections, quantifying the variability in expected strong ground motions at different sites [30]. Their findings highlighted the high seismic risk associated with moderate-sized earthquakes in the NCR and provided insights into reducing the potential damage through appropriate preparedness and mitigation measures [8]. Another analysis of the source characteristics of two small earthquakes in Delhi (M_w 3.4 and M_w 2.6) assessed the potential ground motion from future moderate, local events, indicating that even minor earthquakes can provide valuable information about seismic activity and expected ground

movements [7]. The study concluded that minor earthquakes could cause significant ground shaking, especially in areas with soft soil and high population density, highlighting the need for effective seismic risk management strategies. Investigating the liquefaction potential in Delhi, another study focused on soil samples, borehole logs, and in-situ test findings from various locations, revealing that areas with loose, sandy soils and high-water tables, particularly in the Yamuna River floodplains, are highly susceptible to liquefaction [53,65]. The researchers developed comprehensive maps indicating the liquefaction potential in different zones, which are essential for urban planning and risk reduction measures [17]. The study emphasized the need for strict building codes and construction practices that account for liquefaction risks to enhance earthquake resilience. Using a deterministic approach, a study analysed the seismic hazard in Delhi, incorporating the latest earthquake data and seismic sources within a 300 km radius [51]. By considering ten distinct attenuation correlations, the study highlighted the increased seismic risk in densely populated areas, especially those with older, poorly constructed buildings [56-61]. The findings stressed that the growing population and rapid urbanization in Delhi heighten the city's vulnerability to seismic hazards, necessitating robust mitigation strategies [27]. Employing a modified gridded seismicity model to map the seismic hazard in the National Capital Region (NCR) of India, which includes the NCT of Delhi, another study used an earthquake catalogue of 1,077 events from 1720 to 2015 to estimate seismicity rates and forecast future events [18]. The PSHA produced hazard maps showing expected ground shaking levels for different return periods30. The study concluded that comprehensive seismic risk reduction techniques are essential for the NCR [52]. The approach used in this study to estimate the seismic hazard parameters is shown in Fig.2.

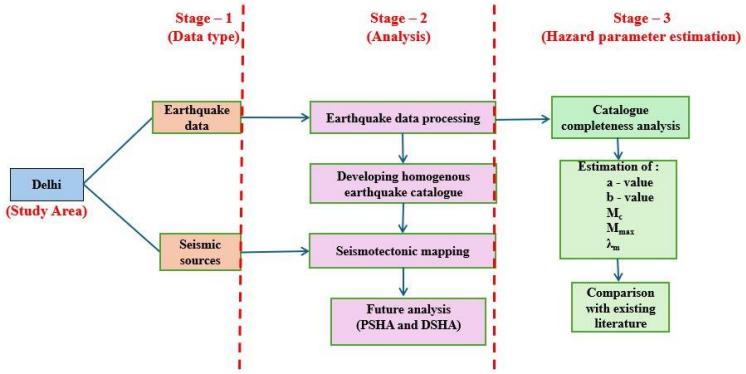

Fig.2: Methodology adopted in this study to estimate the seismic hazard parameters

3. Tectonic setup of the study area and data collection

About 350 km from Delhi, the tectonic environment is shaped by the Himalayas, influenced by the collision of the Indian Plate and the Eurasian Plate. This tectonic collision has created significant geological structures, such as the Main Boundary Thrust (MBT) and the Main Central Thrust (MCT), which are zones of intense deformation and seismic activity [37]. The region experiences frequent earthquakes due to the compressional forces from the converging plates, leading to a landscape marked by folded and faulted rock formations [38]. This tectonic activity has shaped the physical geography and presents seismic hazards, affecting the region's stability and development [13,44].

To understand the seismicity and sesimotectonic more deeply, it is crucial to map seismic sources and associated earthquakes of the region [31]. Characterizing a region's seismicity often involves studying an extended area of 350 to 500 km, with a 500 km radius preferred for low to medium seismic regions.

Since Delhi area falls under seismic zone IV, a 350 km radius from Delhi has been considered, as shown in Fig. 1. Analyzing past earthquake damage helps predict seismic vulnerability [62]. For this study, earthquake data was compiled from sources like the United States Geological Survey, Geological Survey of India, National Center for Seismology [23], Indian Metrological Department [21], Amateur Seismic Centre, and etc [46]. along with pre-instrumental data from existing literature. This compilation created an earthquake catalogue with 855 events over 224 years (1800 AD to May 2024). The data includes earthquake time, latitude, longitude, magnitude (in scales such as I, mb, M_L, Ms, and M_w), and focal depth [32]. Duplicate reports of the same events were noted, and only the maximum magnitude of such events are used for further analysis [68]. A homogeneous earthquake catalogue has been developed by converting different magnitude scales to M_w, since M_w does not saturate for large earthquakes and provides an accurate representation of an earthquake's size47. Magnitude conversions were done using accepted relationships: intensity scales to M_w with G-R's relationship (eq.1) [19,20], mb and M_s scales to M_w with Scordilis' empirical relationships [66] (eq. 2 and 3, 4), and M_L to M_w using the relationship (eq.5) suggested by Sreevalsa et al., [31]. The final homogeneous catalogue consists of 574 events, all with M_w greater than 3.0.

$$M_w = \frac{2}{3} I + 1 \quad (1)$$

$$M_w = 0.85(\pm 0.04)m_b + 1.03(\pm 0.23) \text{ for } 3.5 \leq m_b \leq 6.2 \quad (2)$$

$$M_w = 0.67(\pm 0.05)M_S + 2.07(\pm 0.03) \text{ for } 3 \leq M_S \leq 6.1 \quad (3)$$

$$M_w = 0.99(\pm 0.02)M_S + 0.08(\pm 0.13) \text{ for } 6.2 \leq M_S \leq 8.2 \quad (4)$$

$$M_w = 0.883(\pm 0.054)M_L + 0.585(\pm 0.220)R^2 = 0.762 \quad (5)$$

Earthquakes are categorized into independent and dependent events. Independent events, caused by tectonic loading, are known as background earthquakes or mainshocks [42]. Dependent events, triggered by stress changes in the earth's crust, are referred to as foreshocks or aftershocks [15]. The process of distinguishing dependent events from main events, known as seismicity declustering, eliminates dependent events to create an accurate earthquake catalogue [12,76]. Dependent events are typically smaller and release less energy than main event. Hence, only main events are considered when calculating seismic hazard intensity [33]. Most of the analyses assume a Poisson distribution for the earthquake catalogue, reflecting a model with no memory of time, size, or location [75]. The stochastic declustering technique, based on probability laws, is used to separate dependent events16. Algorithms like the dynamic windowing method by Gardner and Knopoff [14] designate dependent events using time and space windows, but do not consider higher-order aftershocks. Uhrhammer's [74] modification retains the most prominent event within a window and provides spatial and temporal parameters for declustering [67]. Reasenberg's [55] static window test considers events within 30 km and 30 days of a main event as related (eq.6). In this study, Reasenberg's [55] algorithm was used to remove dependent events from the catalogue, reducing it by 32.87%, resulting in a final catalogue of 574 events. The spatial distribution of earthquake events with respect to time and depth is shown in Figs. 3 and 4, and the details of earthquakes with Mw ≥ 6.0 summarized in Table 1.

$$\text{Distance, R (km)} = e^{-1.024+0.804M} \text{ and Time, t(days)} = e^{-2.87+1.235M} \quad (6)$$

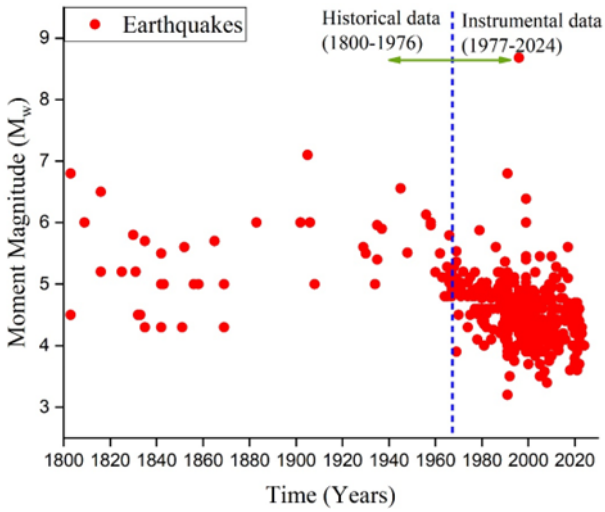

Fig.3: Spatial distribution of earthquake catalogue over the period of 224 years

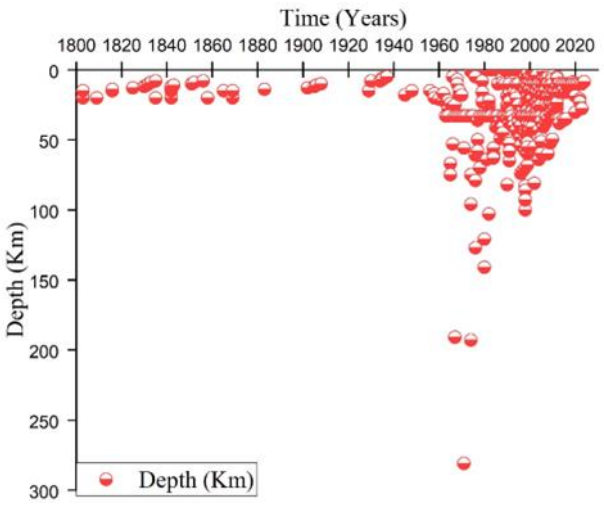

Fig.4: Hypocentres of the earthquakes showing the variation over the period of 224 years

Table 1: Details of major earthquakes of $M_w \geq 6.0$

Year	Date and Time					Lat.	Lon.	Depth (km)	M_w	Source
	Month	Date	Hour	Minutes	Seconds					
1809	9	2	10	0	0	30	79.00	12	6	USGS
1883	5	30	0	0	0	29.4	79.60	0	6	Bhuvan
1902	6	16	0	0	0	31	79.00	0	6	Bhuvan
1906	6	13	0	0	0	31	79.00	0	6	USGS
1958	12	31	3	45	0	30.09	79.86	11	6	USGS
1999	3	28	19	4	0	30.72	75.13	0	6	USGS
1956	10	10	15	31	34	28.5	78.00	0	6.1	CGS
1999	3	28	19	5	12	30.51	79.42	20	6.3	ISC
1816	5	26	0	0	0	30	80.00	0	6.5	USGS
1945	6	4	12	9	6	30	80.00	35	6.5	GR
1803	9	1	0	0	0	27.5	77.70	0	6.8	USGS
1991	10	19	21	23	14	30.78	78.77	10.3	6.8	USGS
1905	9	26	1	26	0	29	74.00	0	7.1	USGS
1996	7	3	10	49	47	30	80.00	17	8.6	ISC

4. Seismotectonic mapping of the Delhi

The region within a 350 km radius of Delhi exhibits complex geological and structural features essential for seismotectonic mapping. This area is characterized by diverse tectonic settings, including the convergence zone between the Indian Plate and the Eurasian Plate, resulting in significant seismic activity [69]. Major fault lines such as the Mahendragarh-Dehradun fault, Sohna fault, and the Delhi-Haridwar ridge, along with the Himalayan frontal thrust, contribute to the area's seismicity34,35. The structural geology is marked by extensive folding and faulting, with prominent anticlines, synclines, and various fault types (normal, reverse, and strike-slip). Key seismic sources, including the MBT and MCT, require detailed analysis. To prepare the seismotectonic map of the study region, geological

features, earthquake data, and seismic sources like faults, active faults, and fault tectonics are analysed. Initially, the complete earthquake catalogue is divided into four groups such as $3.0 \leq M_w \leq 3.99$, $4.0 \leq M_w \leq 4.99$, $5.0 \leq M_w \leq 5.99$, and $M_w \geq 6.0$. Shapefiles for each group are created and overlaid on the seismic sources using GIS. The detailed seismotectonic map of the study region is shown in Figure 5, with active fault details summarized in Table 2. Active faults in the region include the Pawalgarh Fault, Kotabag Fault, Yamuna Tear, and Kala Amb Tear Fault [11]. Understanding these geological and structural elements is crucial for accurately mapping the seismotectonic landscape, guiding earthquake engineering efforts to mitigate risks, and enhancing structural resilience.

Table 2: Details of active faults over the study area

Name of the fault	Description	Field-SEISAT map details	Source	Number on seismotectonic map
Pawalgarh Fault	Active fault studies in the Himalayan Frontal belt between Kosi and Gaula rivers, Nainital district, Uttarakhand	2004-06	GSI, NRO, Lucknow	AF-1
Kotabag Fault		2004-06	GSI, NRO, Lucknow	AF-2
Yamuna Tear	Active Fault study in the Yamuna Tear Zone	2001-03	GSI, NRO, Lucknow	AF-3
Kala Amb Tear Fault	Active fault studies in Himalayan Frontal Belt in Kala Amb area, Himachal Pradesh and Haryana	2010-13	GSI, NRO, Lucknow	AF-4

5. Catalogue completeness analysis

The analysis of earthquake catalogue completeness is crucial for accurate seismic hazard studies. The earthquake data are categorized into four magnitude ranges: $3.0 \leq M_w \leq 3.99$, $4.0 \leq M_w \leq 4.99$, $5.0 \leq M_w \leq 5.99$, and $M_w \geq 6.0$, spanning the available historical record as shown in Table 3. It is evident that data before 1976 likely suffer from underreporting due to limited observational capabilities at that time, highlighting the necessity of completeness analysis, as illustrated in Fig. 3. To ensure the catalogue's completeness, two methods are employed: the Cumulative Visual Inspection (CUVI) method [43] and Stepp's method [70]. CUVI, proposed by Mulargia and Tinti [43], is a graphical technique that involves plotting the cumulative number of earthquakes against the time duration [73]. The portion of the plot where the rate of earthquake events remains constant indicates catalogue completeness, effectively identifying periods where data recording is consistent and reliable [71]. In this analysis, the earthquake catalogue is subdivided by magnitude intervals starting from M_w 3.0 with increments of magnitude 1.0. By examining these subdivisions, the period of completeness can be accurately determined, ensuring a comprehensive record of seismic activity. The completeness period of the earthquake catalogue using CUVI method is shown on Fig. 6.

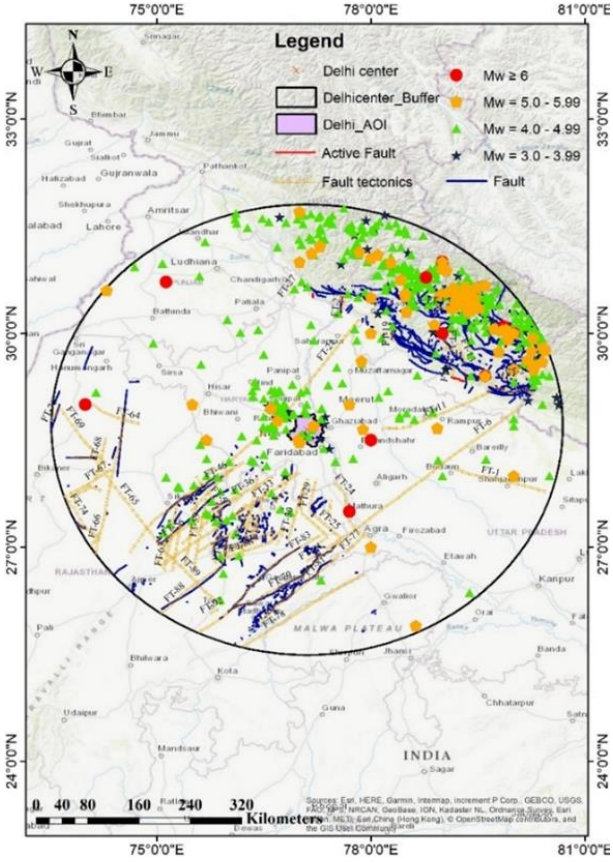

Fig.5: Seismotectonic mapping of the study area

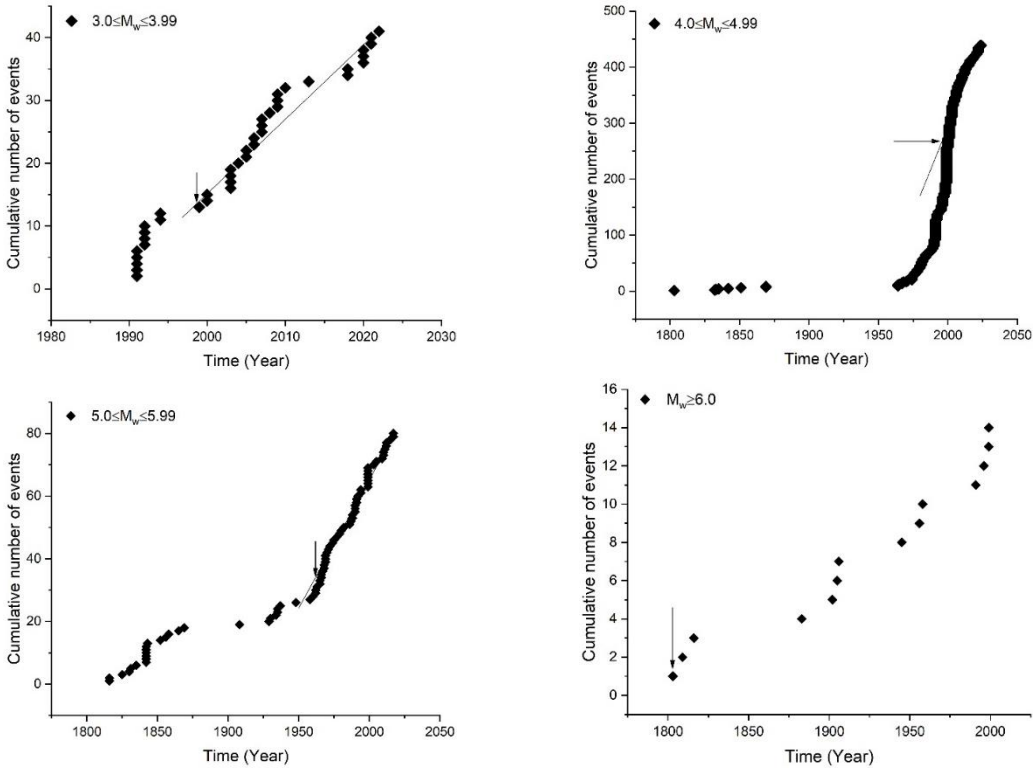

Fig.6: Completeness period using CUVI method

The Stepp method [70] facilitated completeness analysis by assuming earthquake data within each magnitude class follow a Poisson process, where events occur independently at a constant mean rate. This method leverages the inverse relationship between variance and sample size: larger samples, indicating more comprehensive reporting, yield reduced variance. For datasets with significant incompleteness, the Stepp method groups earthquake data into magnitude classes, treating each class as a temporal point process. This statistical approach benefits from variance reduction in sample mean estimates proportional to the number of observations. This allows for minimizing variance by increasing the sample size, if reporting is temporally complete, and the process is stationary, meaning that mean variance and other moments remain constant across observations. The Poisson distribution models the earthquake sequence, with the mean rate per unit time interval denoted as λ, and its variance given by: The mean rate (λ) and its variance (σ^2) of earthquake occurrences are estimated using the following equations.

$$\lambda = \frac{1}{n}\sum_{i=1}^{n} x_i \tag{7}$$

$$\sigma_\lambda^2 = \frac{\lambda}{n} \tag{8}$$

Where n is the number of unit time intervals. Taking the unit time interval as one year, the formula becomes:

$$\sigma_\lambda = \sqrt{\lambda}/\sqrt{T} \tag{9}$$

where T is the sample length. The variance behaves as $1/\sqrt{T}$ in subintervals where the mean rate of occurrence in a magnitude class is constant. Stability in occurrence rate is expected in subintervals long enough to estimate the mean accurately but short enough to exclude incomplete reports. Table 4 lists the rate of earthquake occurrence (N/T) for different magnitude ranges over time intervals, where N is the cumulative number of earthquakes, and T is the time interval. These data help determine the standard deviation of the mean estimate using the formula above, with results illustrated in Fig. 7. Both table 4 and Fig.7 highlight critical features for the statistical treatment of earthquake data. Regardless of using empirical relationships like N = [a – bM] with extreme value distribution, each magnitude interval's plotted points should form a straight line if the data set is complete. The line slopes for all magnitude intervals should be identical, reflecting the region's seismicity. The obtained completeness period of the catalogue is summarised in Table 5.

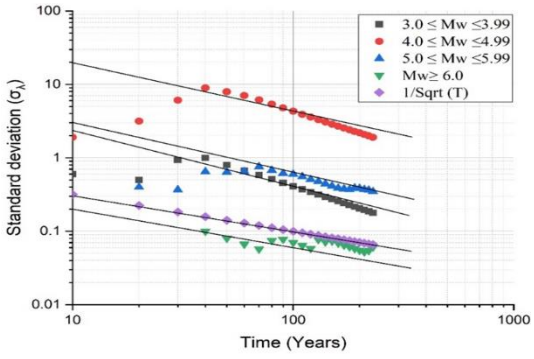

Fig.7: Analyzing annual events by sample length and magnitude class in study region

Table 3: Decadal earthquake counts by M_w ranges from 1800

Time (span)	Magnitude classes				Total	Cumulative of events
	$3.0 \leq M_w \leq 3.99$	**$4.0 \leq M_w \leq 4.99$**	**$5.0 \leq M_w \leq 5.99$**	**$M_w \geq 6.0$**		
2020 - 2029	6	19	-	-	25	25
2010 - 2019	4	44	8	-	56	81
2000 - 2009	18	12-	3	-	141	222
1990 - 1999	12	176	15	4	207	429
1980 - 1989	-	39	6	-	45	474
1970 - 1979	-	25	7	-	32	506
1960 - 1969	1	8	14	-	23	529
1950 - 1959	-	-	1	2	3	532
1940 - 1949	-	-	1	1	2	534
1930 - 1939	-	-	5	-	5	539
1920 - 1929	-	-	1	-	1	540
1910 - 1919	-	-	-	-	-	540
1900 - 1909	-	-	1	3	4	544
1890 - 1899	-	-	-	-	-	544
1880 - 1889	-	-	-	1	1	545
1870 - 1879	-	-	-	-	-	545
1860 - 1869	-	2	2	-	4	549
1850 - 1859	-	1	3	-	4	553
1840 - 1849	-	1	7	-	8	561
1830 - 1839	-	3	3	-	6	567
1820 - 1829	-	-	1	-	1	568
1810 - 1819	-	-	2	1	3	571
1800 - 1809	-	1	-	2	3	**574**
Total	**41**	**439**	**80**	**14**	**574**	

Table 4: Earthquake occurrence rates (N/T) by magnitude, aiding variance estimation

Time span	Time interval	3.0 ≤ Mw ≤3.99		4.0 ≤ Mw ≤4.99		5.0 ≤ Mw ≤5.99		Mw≥ 6.0		Cumulative No. of events
		N	N/T (λ)	N	N/T (λ)	N	N/T (λ)	N	N/T (λ)	
2020 - 2029	10	6	0.60	19	1.90	0	0.00	0	0.00	25
2010 - 2019	20	10	0.50	63	3.15	8	0.40	0	0.00	81
2000 - 2009	30	28	0.93	183	6.10	11	0.37	0	0.00	222

1990 - 1999	40	40	1.00	359	8.98	26	0.65	4	0.10	429
1980 - 1989	50	40	0.80	398	7.96	32	0.64	4	0.08	474
1970 - 1979	60	40	0.67	423	7.05	39	0.65	4	0.07	506
1960 - 1969	70	41	0.59	431	6.16	53	0.76	4	0.06	529
1950 - 1959	80	41	0.51	431	5.39	54	0.68	6	0.08	532
1940 - 1949	90	41	0.46	431	4.79	55	0.61	7	0.08	534
1930 - 1939	100	41	0.41	431	4.31	60	0.60	7	0.07	539
1920 - 1929	110	41	0.37	431	3.92	61	0.55	7	0.06	540
1910 - 1919	120	41	0.34	431	3.59	61	0.51	7	0.06	540
1900 - 1909	130	41	0.32	431	3.32	62	0.48	10	0.08	544
1890 - 1899	140	41	0.29	431	3.08	62	0.44	10	0.07	544
1880 - 1889	150	41	0.27	431	2.87	62	0.41	11	0.07	545
1870 - 1879	160	41	0.26	431	2.69	62	0.39	11	0.07	545
1860 - 1869	170	41	0.24	433	2.55	64	0.38	11	0.06	549
1850 - 1859	180	41	0.23	434	2.41	67	0.37	11	0.06	553
1840 - 1849	190	41	0.22	435	2.29	74	0.39	11	0.06	561
1830 - 1839	200	41	0.21	438	2.19	77	0.39	11	0.06	567
1820 - 1829	210	41	0.20	438	2.09	78	0.37	11	0.05	568
1810 - 1819	220	41	0.19	438	1.99	80	0.36	12	0.05	571
1800 - 1809	230	41	0.18	439	1.91	80	0.35	14	0.06	574

Table 5: Completeness period for different magnitude ranges from CUVI [43] and Stepp's method [70].

Magnitude range	CUVI method		Stepp's method	
	Completeness period	Time interval (years)	Completeness period	Time interval (years)
$M_w = 3.0 \leq M_w \leq 3.99$	1997-2024	27	1984-2024	40
$M_w = 4.0 \leq M_w \leq 4.99$	1994-2024	30	1954-2024	70
$M_w = 5.0 \leq M_w \leq 5.99$	1963-2024	61	1924-2024	100
$M_w \geq 6.0$	1803-2024	221	1894-2024	130

6. Estimation and comparison of seismic hazard parameters

In seismic hazard analysis, evaluating parameters such as a-value, b-value, λ, β, and M_c is crucial for understanding earthquake occurrence patterns [48]. The Gutenberg-Richter (G-R) recurrence relation serves as a fundamental method to estimate these parameters, specifically a and b, which define the annual rate of earthquakes across different magnitudes and describe the seismic activity of a region [49]. This study utilized statistical methods like the Least Squares Method (LSM) and Maximum Likelihood Method (MLM) to calculate these parameters over a determined completeness period identified through the CUVI and Stepp's method50. The LSM divided earthquake magnitudes into groups and used regression analysis to establish relationships between annual earthquake rates and magnitude ranges, yielding a-values of 4.12 (CUVI) and 3.13 (Stepp's), and b-values of 0.83 (CUVI) and 0.65 (Stepp's). The mathematical functional form of the LSM method with obtained values is given below equations 10 (from CUVI) and 11 (from Steep's method). The G-R relation with the estimated seismic hazard parameters is shown in below Fig.8.

$$\log_{10} \lambda_m = 4.12 - 0.83\,M \qquad (10)$$

$$\log_{10} \lambda_m = 3.13 - 0.65\,M \qquad (11)$$

Meanwhile, MLM applied Aki's [2] relation (refer eq. 12) to determine the b-value across the entire magnitude range, with Mc set at 3.5 M_w using the Z-map technique in MATLAB to manage data uncertainties [77]. Furthermore, estimating the maximum credible earthquake (Mmax) is crucial for assessing seismic hazard, providing insights into potential strain release during major earthquakes [72]. Using Gupta's empirical correlations, the expected maximum magnitude is 9.1 based on historical seismic events. This parameter is pivotal for earthquake-resistant design and risk mitigation strategies, offering critical information on the seismic potential of a region.

$$b = \frac{\log_{10(e)}}{[M_{mean} - \left(M_C - \frac{\Delta_{m_{bin}}}{2}\right)]} \qquad (12)$$

Where Mmean denotes the mean magnitude, M_c represents the minimum magnitude within a specific Δm interval. Here, Δm = 0.1 M_w is applied across the entire magnitude spectrum. M_c signifies the lowest recorded magnitude in the region, typically determined by plotting cumulative event numbers against magnitudes.

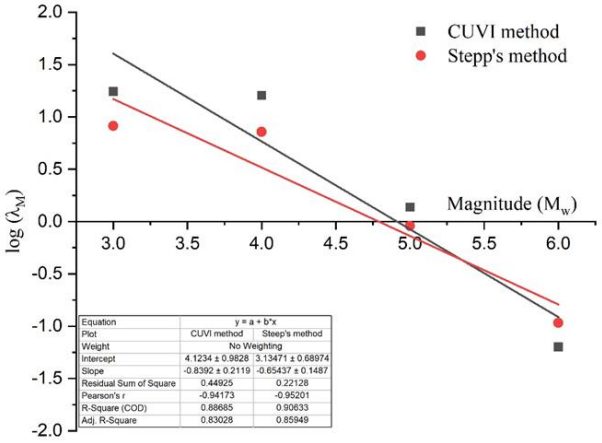

Fig.8: G-R relation showing the hazard parameters for the study region

7. Conclusions

This study investigated the seismicity and seismotectonic of a region within a 350 km radius of Delhi, India. The convergence of the Indian and Eurasian Plates shapes the complex geological and structural setting, leading to significant seismic activity. Major fault lines and prominent folds and thrusts contribute to the region's earthquake susceptibility. A comprehensive earthquake catalogue was developed using data from various sources, spanning over 224 years (1800 AD to May 2024). The catalogue was meticulously curated by converting different magnitude scales to a homogeneous Mw scale and eliminating dependent events (foreshocks and aftershocks) using Reasenberg's declustering technique [55]. To assess the completeness of the catalogue, crucial for reliable seismic hazard studies, we employed the CUVI and Stepp's method. The analysis revealed that pre-1976 data likely suffers from underreporting. The completeness period was determined using both methods, providing a foundation for accurate evaluation of seismic parameters. The G-R recurrence relation was utilized to estimate key parameters like a-value and b-value using the established completeness period. The results provide insights into the regional earthquake occurrence patterns. Furthermore, the maximum credible earthquake (M_{max}) was estimated using incremental method, highlighting the potential for strain release during large earthquakes. This critical information is essential for earthquake-resistant design and risk mitigation strategies. In conclusion, this study has established a comprehensive understanding of the seismicity and seismotectonic of the Delhi region. The analysis of the earthquake catalogue's completeness and the estimation of seismic parameters provide valuable data for future seismic hazard assessments and contribute to improved preparedness for potential earthquakes. The estimated results have been compared with existing literature and found that the obtained b-values in this is reliable and M_{max} is shows slightly higher, this is due to the size of the catalogue, extent of the study region and time span of the data set. Overall, this study offers critical advantages for earthquake risk reduction in Delhi. By creating a high-quality catalogue and assessing its completeness, the study ensures reliable data for future assessments. Furthermore, estimating key parameters like a-value (3.13-4.12), b-value (0.65-0.83), M_c (3.5 M_w), and Mmax (9.1 M_w) provides crucial information for engineers and policymakers to design earthquake-resistant structures and develop effective mitigation strategies. Overall, this work improves understanding of seismic hazards in Delhi, paving the way for better preparedness.

References

[1] Agrawal, S.K. and Chawla, J., Seismic hazard assessment for Delhi region. Current Science, 1717-1724 (2006).
[2] Aki K., Maximum likelihood estimate of b in the formula logN= a-bM and its confidence limits, Bulletin of the Earthquake Research Institute, 43, 237-239 (1965)
[3] Ambraseys, N., Reappraisal of North-Indian earthquakes at the turn of the 20th century. Current Science, 79(9), 1237-1250 (2000).
[4] Arandhakar, S., Chaudhary, N., Depuru, S.R., Dubey, R.K. and Bhukya, M.N., Analysis and implementation of robust metaheuristic algorithm to extract essential parameters of solar cell. IEEE Access, 10 (1), 40079-40092 (2021).
[5] Babu, P.A., Nagaraju, V.S. and Vallabhuni, R.R. Speech emotion recognition system with librosa. In 2021 10th IEEE international conference on communication systems and network technologies (CSNT), IEEE, 421-424, (2021).
[6] Banerjee, S. and Kumar, A., Determination of seismic wave attenuation in Delhi, India, towards quantification of regional seismic hazard. Natural Hazards, 92, 1039-1064 (2018).
[7] Bansal, B.K., Singh, S.K., Dharmaraju, R., Pacheco, J.F., Ordaz, M., Dattatrayam, R.S. and Suresh, G., Source study of two small earthquakes of Delhi, India, and estimation of ground motion from future moderate, local events. Journal of Seismology, 13, 89-105 (2009).
[8] Bhukya, L., Kedika, N.R. and Salkuti, S.R., Enhanced maximum power point techniques for solar photovoltaic system under uniform insolation and partial shading conditions: a review, Algorithms, 15(10), 365-372 (2022).
[9] Bilham, R., Earthquakes in India and the Himalaya: tectonics, geodesy and history. Ann Geophys, 47(3), 839-858 (2004).
[10] Cheruvu, A., Radhakrishna, V. and Rajasekhar, N., Using normal distribution to retrieve temporal associations by Euclidean distance. In 2017 International Conference on Engineering & MIS (ICEMIS), 1-3, IEEE (2017).
[11] Dasgupta S., Narula P.L., Acharyya S.K. and Banerjee J., Seismotectonic atlas of India and its environs, Geological Survey of India (2000)
[12] Devi, M.D., Juliet, A.V., Hariprasad, K., Ganesh, V., Ali, H.E., Algarni, H. and Yahia, I.S., Improved UV Photodetection of Terbium-doped NiO thin films prepared by cost-effective nebulizer spray technique. Materials Science in Semiconductor Processing, 127 (3), 105673-78. (2021).
[13] Gade, M.S.L. and Rooban, S. Run time fault tolerant mechanism for transient and hardware faults in alu for highly reliable embedded processor. In 2020 International Conference on Smart Technologies in Computing, Electrical and Electronics (ICSTCEE), IEEE, 44-49 (2020).
[14] Gardner J.K. and Knopoff L., Is the sequence of earthquakes in Southern California, with aftershocks removed, Poissonian?, Bulletin of the Seismological Society of America, 64(5), 1363-1367 (1974)
[15] Görgün E., Analysis of the b-values before and after the 23 October 2011 Mw 7.2 Van–Erciş, Turkey earthquake, Tectonophysics, 603, 213-221 (2013).
[16] Goud, B.S., Srilatha, P. and Shekar, M.R., Effects of mass suction on MHD boundary layer flow and heat transfer over a porous shrinking sheet with heat source/sink. Int. Journal of Innovative Technology and Exp. Engineering, 8(10), 263-266 (2019).
[17] GovindaRaju, L., Ramana, G.V., HanumanthaRao, C. and Sitharam, T.G., Site-specific ground response analysis. Current Science, 1354-1362 (2004).
[18] Gupta, A., Gupta, I.D. and Gupta, V.K., Probabilistic seismic hazard mapping of National Capital Region of India using a modified gridded seismicity model. Soil Dynamics and Earthquake Engineering, 144, 106632 (2021).
[19] Gutenberg B. and Richter C.F., Frequency of earthquakes in California, Bulletin of the Seismological Society of America, 34(4), 185-188 (1944)
[20] Gutenberg, B., and Richter, C. F., Earthquake magnitude, intensity, energy, and acceleration: (Second paper), Bulletin of the Seismological Society of America, 46 (2), 105–145 (1956).
[21] Indian Meteorological Department (IMD), www.imd.gov.in, New Delhi, India (Through personal communication) (2024)
[22] Indian Standard, IS 1893 (Part I), Criteria for earthquake resistance design of structures, Part-I, Bureau of Indian Standard, New Delhi (2016)
[23] International Seismological Centre, On-line Bulletin, http://www.isc.ac.uk, International Thatcham, United Kingdom (2024)
[24] Iyengar, R.N. and Ghosh, S., Microzonation of earthquake hazard in greater Delhi area. Current Science, 87(9), 1193-1202 (2004).
[25] Iyengar, R.N. and Ghosh, S., Seismic hazard mapping of Delhi city. In Proceedings of 13th world conference on earthquake engineering. Vancouver, BC, Canada. 180, (2004).
[26] Jagadha, S., Gopal, D. and Kishan, N., Nanofluid flow of higher order radiative chemical reaction with effects of melting and viscous dissipation. In Journal of Physics: Conference Series, 1451(1), 012003, IOP Publishing, (2020).

[27] Janakiramaiah, B., Kalyani, G., Prasad, L.V., Karuna, A. and Krishna, M., Intelligent system for leaf disease detection using capsule networks for horticulture. Journal of Intelligent and Fuzzy Systems, 41(6), 6697-6713 (2021)
[28] Jayanthi, N., Lakshmi, A., Raju, C.S.K. and Swathi, B. December. Dual translation of international and Indian regional language using recent machine translation. In 2020 3rd International Conference on Intelligent Sustainable Systems (ICISS), IEEE, 682-686, (2020).
[29] Kalyani, G., Janakiramaiah, B., Karuna, A., and Prasad, L.N., Diabetic retinopathy detection and classification using capsule networks. Complex and Intelligent Systems, 9(3), 2651-2664 (2023).
[30] Kiran Prakash, K., Nishanth Kiran, D., Madhu Sudhan Reddy, M., Khan, M.M. and Gonavaram, K.K., Local Site Effects and Liquefaction Analysis of Multilayered Soil. In Proceedings of the Indian Geotechnical Conference 2019: IGC-2019, Springer Singapore, IV, 533-544 (2021).
[31] Kolathayar S., Sitharam T.G. and Vipin K.S., Spatial variation of seismicity parameters across India and adjoining areas, Natural Hazards, 60(3), 1365-1379 (2012)
[32] Kumar, C.L., Jayakumar, V., and Bharathiraja, G., Optimization of welding parameters for friction stir spot welding of AA6062 with similar and dissimilar thicknesses. Materials Today: Proceedings, 19(1), 251-255 (2019).
[33] Kumar, K.U., Babu, P., Basavapoornima, C., Praveena, R., Rani, D.S. and Jayasankar, C.K., Spectroscopic properties of Nd3+-doped boro-bismuth glasses for laser applications, Physica B: Condensed Matter, 646(1),414327 (2022).
[34] Kumar, N. R., Goud, S. J., Srilatha, P., Manjunatha, P.T., Rani, S.P., Kumar, R., and Suresha, S., Cattaneo–Christov heat flux model for nanofluid flow over a curved stretching sheet: An application of Stefan blowing. Heat Transfer, 51(6), 4977-4991 (2022).
[35] Lakshmi, L., Reddy, M.P., Santhaiah, C. and Reddy, U.J., Smart phishing detection in web pages using supervised deep learning classification and optimization technique ADAM, Wireless Personal Communications, 118(4), 3549-3564 (2021).
[36] Madhusudhan Reddy, M., Rajasekhara Reddy, K. and Kalyan Kumar, G., Seismic source characterization for Amaravati capital region, Andhra Pradesh, India. In Seismic Hazards and Risk: Select Proceedings of 7th ICRAGEE 2020, Springer Singapore, 87-94 (2021).
[37] Mahajan, A.K., Thakur, V.C., Sharma, M.L. and Chauhan, M., Probabilistic seismic hazard map of NW Himalaya and its adjoining area, India. Natural Hazards, 53, 443-457 (2010).
[38] Malliga, S., Prasad. N., L.V., Janakiramaiah B., Mohan Babu A., and Sathishkumar, V.E. Hyperparameter Optimization for Transfer Learning of VGG16 for Disease Identification in Corn Leaves Using Bayesian Optimization, Big Data, 10(3), 215-229 (2022).
[39] Mandal, H.S., Jani, A. and Mishra, O.P., A Detail Probabilistic Seismic Hazard Analysis of National Capital Territory of Delhi, India (2022).
[40] Mandapudi, S., Chaganti, S.S., Gorle, S., Prasad, S.U., Govardhan, D., and Praveen, B., CFD simulation of flow past wing body junction: a 3-D approach. International Journal of Mechanical and Production Engineering Research and Development, 7(4), 341-350 (2017).
[41] Mohanty, W.K., Walling, M.Y., Nath, S.K. and Pal, I., First order seismic microzonation of Delhi, India using geographic information system (GIS). Natural Hazards, 40, 245-260 (2007).
[42] Molchan G.M. and Dmitrieva O.E., Aftershock identification: methods and new approaches, Geophysical Journal International, 109(3), 501-516 (1992)
[43] Mulargia F. and Tinti S., Seismic sample areas defined from incomplete catalogues: An application to the Italian territory, Physics of the Earth and Planetary Interiors, 40(4), 273-300 (1985)
[44] Muthuganeisan P. and Raghukanth S.T.G., Site-specific probabilistic seismic hazard map of Himachal Pradesh, India, Part II, Hazard estimation, Acta Geophysica, 64(4), 853-884 (2016)
[45] Nath, S.K. and Thingbaijam, K.K.S., Probabilistic seismic hazard assessment of India. Seismological Research Letters, 83(1), 135-149 (2012).
[46] National Earthquake Information Center (NEIC), Online earthquake catalogue, (http://earthquake.usgs.gov/earthquakes) (2024)
[47] Padmaja, B., Prasad, V.R., and Sunitha, K.V.N., A machine learning approach for stress detection using a wireless physical activity tracker. International Journal of Machine Learning and Computing, 8(1), 33-38 (2018).
[48] Priyamvada S., Seismic Energy and b-value for Garhwal Himalayas, India, Disaster Advances, 11(7), 13-16 (2018)
[49] Radhakrishna, V., Kumar, P.V., Janaki, V. and Rajasekhar, N., Estimating prevalence bounds of temporal association patterns to discover temporally similar patterns, Advances in Intelligent Systems and Computing, 576(2), 209-220 (2017).
[50] Raghukanth S.T.G., Seismicity parameters for important urban agglomerations in India, Bulletin of Earthquake Engineering, 9(5), 1361-1386 (2011)
[51] Ramkrishnan, R., Kolathayar, S. and Sitharam, T.G., Deterministic seismic hazard analysis of north and central Himalayas using region-specific ground motion prediction equations. Journal of Earth System Science, 130(4), 232 (2021).

[52] Ramu, G., A secure cloud framework to share EHRs using modified CP-ABE and the attribute bloom filter. Education and Information Technologies, 23(5), 2213-2233 (2018).
[53] Rao, K.S. and Rathod, G.W., Seismic microzonation of Indian megacities: a case study of NCR Delhi. Indian Geotechnical Journal, 44, 132-148 (2014).
[54] Rathje, E., Pehlivan, M., Gilbert, R. and Rodriguez-Marek, A., Incorporating site response into seismic hazard assessments for critical facilities: A probabilistic approach. Perspectives on earthquake geotechnical engineering: In honour of Prof. Kenji Ishihara, 93-111 (2015).
[55] Reasenberg P., Second-order moment of central California seismicity, 1969-1982, Journal of Geophysical Research: Solid Earth, 90(7), 5479-5495 (1985)
[56] Reddy, M., Ch, H.R., Rajashekara Reddy, K. and Kumar, K., Seismic Site Classification and Ground Response Analysis of Amaravati Region, Andhra Pradesh, India. Disaster Advances, 14(3), 10-20 (2021).
[57] Reddy, M., Konda, R.R., Kumar, G.K. and Asadi, S.S., Site characterization and evaluation of seismic sources for Amaravati region. International Journal of Geotechnical Earthquake Engineering (IJGEE), 11(1), 71-86 (2020).
[58] Reddy, M., Rajashekara Reddy, K., Ch, H.R. and Kumar, K., Evaluation and comparison of seismic hazard parameters for Amaravati Region. Disaster Advances, 13(8), pp.11-22 (2020).
[59] Reddy, M.M., Rao, C.H., Reddy, K.R. and Kumar, G.K., Deaggregation of seismic hazard for Amaravati capital region in Peninsular India. Asian Journal of Civil Engineering, 24(4), 1077-1095 (2023).
[60] Reddy, M.M., Rao, C.H., Reddy, K.R. and Kumar, G.K., Site-specific ground response analysis of some typical sites in Amaravati region, Andhra Pradesh, India. Indian Geotechnical Journal, 52(1), 39-54 (2022).
[61] Reddy, M.M., Siddhardha, R., Kumar, G.K. and Suresh, R., Applications of GIS in Estimating the Probable Maximum Earthquake Magnitude for Amaravati Region, Andhra Pradesh, India. In International Virtual Conference on Developments and Applications of Geomatics, Singapore: Springer Nature Singapore 15-24 (2022)
[62] Rizwana, M.S., and Sarah, P., Impedance and electromechancial studies on Ca0. 1Sr0. 9LaxBi2-xTa2O9 ceramics. Ferroelectrics, 524(1), 95-101 (2018).
[63] Sandhu, M., Sharma, B., Mittal, H., Yadav, R.B.S., Kumar, D. and Teotia, S.S., Simulation of strong ground motion due to active Sohna fault in Delhi, National Capital Region (NCR) of India: an implication for imminent plausible seismic hazard. Natural Hazards, 104(3), 2389-2408 (2020).
[64] Sastry, Y.S., Budarapu, P.R., Krishna, Y. and Devaraj, S., Studies on ballistic impact of the composite panels. Theoretical and Applied Fracture Mechanics, 72(1), 2-12 (2014).
[65] Satyam, D.N. and Rao, K.S., Liquefaction hazard assessment using SPT and VS for two cities in India. Indian Geotechnical Journal, 44, 468-479 (2014).
[66] Scordilis E.M., Empirical global relations converting MS and mb to moment magnitude, Journal of Seismology, 10(2), 225-236 (2006)
[67] Shejkar, S.K., Agrawal, B., Agrawal, A., Gupta, G., and Pati, P.R., Influence of filler content and surface modification on physical and mechanical properties of epoxy/walnut shell particulate composites, Journal of Adhesion Science and Technology, 37(7), 1215-1232 (2023).
[68] Siddhardha, R., Reddy, M.M., Kiran, R. and Kumar, G.K., Seismotectonic mapping and energy release analysis for Ongole city of Andhra Pradesh, India. Disaster Advances, 16(11), pp.40-52. (2023)
[69] Spandana, K., and Rao, V.S., Internet of Things (Iot) Based smart water quality monitoring system. International Journal of Engineering and Technology (UAE), 7(3), 259-262 (2018).
[70] Stepp J.C., Analysis of completeness of the earthquake sample in the Puget Sound area and its effect on statistical estimates of earthquake hazard, In Proc. of the 1st Int. Conf. on Microzonazion, Seattle, 2, 897-910 (1972)
[71] Telagam, N., Kandasamy, N., and Nanjundan, M., Smart sensor network based high quality air pollution monitoring system using labview. International Journal of Online Engineering, 13(08), 79-87 (2017).
[72] Thingbaijam K.K.S. and Nath S.K., Estimation of maximum earthquakes in northeast India, Pure and Applied Geophysics, 165(5), 889-901 (2008)
[73] Tinti S. and Mulargia F., Effects of magnitude uncertainties on estimating the parameters in the Gutenberg-Richter frequency magnitude law, Bulletin of the Seismological Society of America, 75(6), 1681-1697 (1985)
[74] Uhrhammer R.A., Characteristics of northern and central California seismicity, Earthquake Notes, 57(1), 21 (1986)
[75] Vallabhuni, R.R., Lakshmanachari, S., Avanthi, G., and Vijay, V., Smart cart shopping system with an RFID interface for human assistance. In 2020 3rd International Conference on Intelligent Sustainable Systems (ICISS) 165-169, IEEE, (2020).
[76] Van Stiphout T., Zhuang J. and Marsan D., Seismicity declustering, Community Online Resource for Statistical Seismicity Analysis, available at http://www.corssa.org, doi: 10.5078/corssa-52382934 (2012)
[77] Wiemer S., A software package to analyze seismicity: ZMAP, Seismological Research Letters, 72(3), 373-382 (2001)